Langmuir

ARTICLE

pubs.acs.org/Langmuir

Surface Phase Behavior and Domain Topography of Ascorbyl Palmitate Monolayers

Luciano Benedini,[†] Maria Laura Fanani,*[,‡] Bruno Maggio,[‡] Natalia Wilke,[‡] Paula Messina,[†] Santiago Palma,[§] and Pablo Schulz[†]

[†]Instituto de Química del Sur (INQUISUR−CONICET), Departamento de Química, Universidad Nacional del Sur, 8000FTN Bahía Blanca, Argentina

[‡]Centro de Investigaciones en Química Biológica de Córdoba (CIQUIBIC−CONICET), Departamento de Química Biológica, Facultad de Ciencias Químicas, Universidad Nacional del Córdoba, Haya de la Torre y Medina Allende, Ciudad Universitaria, X5000HUA Córdoba, Argentina

[§]Departamento de Farmacia, Facultad de Ciencias Químicas, Universidad Nacional de Córdoba, Ciudad Universitaria, X5000HUA Córdoba, Argentina

ABSTRACT: Ascorbyl palmitate (ASC_{16}) is a molecule of potential pharmacological interest due to its antioxidant properties and amphiphilic nature. The surface behavior of ASC_{16} was studied using Langmuir monolayers and Brewster angle microscopy. This molecule formed stable monolayers at room temperature that showed phase transition from a liquid-expanded to liquid-condensed or crystalline phase, depending on the subphase conditions. Using a theoretical approach, we were able to explain the behavior of the ASC_{16} film at different bulk pH values and salt conditions based on the surface pH and the dissociation fraction of the film. Both condensed phases corresponded to highly packed conditions with the crystalline phase occurring at a low charge density, showing molecular tilting and preferential growth at characteristic angles, while the liquid-condensed phase formed in highly charged surfaces revealed small flowerlike domains probably as a consequence of internal dipole repulsion. A smaller perpendicular dipole moment was observed for the crystalline than the liquid-condensed phase which may explain the domain features. In conclusion, ASC_{16} showed a complex surface behavior that was highly sensitive to subphase conditions.

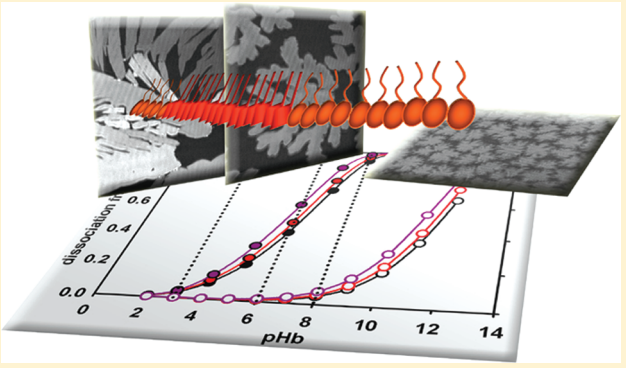

1. INTRODUCTION

Vitamin C (L-ascorbic acid) is a strong and powerful water-soluble nonenzymatic antioxidant that efficiently protects biological molecules against oxidative degradation. It also shows synergistic effects with other antioxidants such as tocopherols and β-carotenoids, by establishing a particular recycling system,[1] and improves the elasticity of the skin thus reducing wrinkles by stimulating collagen synthesis.[2] As a consequence of these favorable effects, vitamin C has long been used in pharmaceutical and cosmetic preparations.[3] Nevertheless, its low stability is a serious limitation. With it being easily oxidized, especially under aerobic conditions and light exposure, resulting in it being degraded first in a reversible step to dehydroascorbic acid and second irreversibly to oxalic acid.[4] To minimize the problem of stability, derivatives of vitamin C have been synthesized that have a similar action to ascorbic acid but with improved chemical stability.[5]

Of the vitamin C derivatives, alkanoyl-6-*O*-ascorbic acid esters (ASC_n) have been of particular interest, because of their lipophilic character favoring their ability to penetrate into the membranes.[6,7] Since a hydrophobic portion (alkyl chain) and a polar group (ascorbic acid) are present in their structures, such esters behave as amphiphilic molecules. In order to transfer these particular antioxidant properties of vitamin C to lipophilic media, several alkanoyl-6-*O*-ascorbic acid esters have been synthesized and characterized.[8−12] The solubility of these ASC_n decreased with the alkyl chain length (n) and increased with temperature with these compounds forming transparent dispersions in water above the critical micellar concentration (CMC) and critical micellar temperature (CMT).[12] If these dispersions are cooled down to below CMT, a semicrystalline mesophase (coagel) is obtained. Then, on heating, coagels form either liquid or homogeneous micelar structures ($n \leq 10$) or gels ($n \geq 11$), depending on the chain length, temperature, and the addition of other solutes. The phase behavior of coagels as a function of the alkyl chain length was previously investigated.[9] These coagel systems were found to be able to substantially increase the apparent solubility[10] and the stability of certain drugs.[11] They therefore

Received: May 17, 2011
Revised: July 15, 2011
Published: July 18, 2011

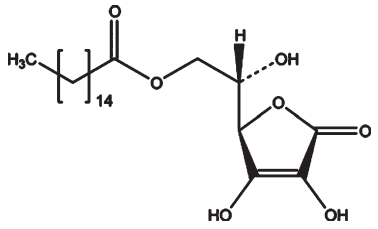

Figure 1. Chemical structure of ASC_{16}.

present a promising tool as drug carriers in pharmaceutical dosage formulations.

The aim of this Article is to study the surface behavior of ascorbyl palmitate (ASC_{16}, see Figure 1) in Langmuir monolayers. The ascorbic acid molecule contains four hydroxyl groups in positions 2, 3, 5, and 6; the OH groups in positions 2 and 3 have pK_a = 11.6 and 4.2, respectively, while those in positions 5 and 6 behave as secondary and primary alcohol residues, respectively, and carbon 4 is chiral. The ascorbate ring undergoes a tautomeric equilibrium with the C_1═O and C_3−OH groups interchanging the double bond[13] with this structure favoring interfacial H-bonding formation between the polar headgroup and the water subphase, as well as between polar groups of neighboring ASC_{16} molecules.

The behavior of ASC_{16} could be expected to be similar to that of the nonionic surfactant dodecanephosphonic acid,[14,15] whose pK_a values are 2.80 and 8.40; however, previous evidence shows that ASC_{16} behaves as an anionic surfactant.[16] Thus, at pH ≈ 6, the ascorbic ring is negatively charged when it is as a monomer. Moreover, if ASC_{16} molecules self-assemble in a surface (as is the case in Langmuir monolayers), the dissociation of the acidic C_3−OH group should lead to a negatively charged surface and, consequently, to a double layer of ions close to the interface. Therefore, protons will also be attracted to the surface and the surface pH (pH_s) will be lower than the bulk pH (pH_b),[17] thus affecting the ionization of ASC_{16}.

In this work, we studied the effect of subphase salt content and pH on the phase state and surface topography of ASC_{16} monolayer from both a theoretical and experimental approach. Parameters such as temperature, surface pressure, mean molecular area, surface potential, compressibility, and topography were directly measured and analyzed from compression isotherms and Brewster angle microscopy experiments. The dissociation degree of the C_3−OH group, pH_s and salt effect, and the surface potential difference due to the ionic double layer are estimated theoretically. The information gathered contributes to the understanding of the complex surface behavior of ASC_n.

2. EXPERIMENTAL SECTION

2.1. Materials. Ascorbyl palmitate (ASC_{16}) was purchased from Fluka (Italy) (MW 414.53). All the reagents were of analytical grade (99% pure) and used without further purification. Solvents were of the highest commercial purity available. The water was purified by using a Milli-Q (Millipore, Billerica, MA) system, which yelded a product with a resistivity of ∼18.5 MΩ/cm. The absence of surface-active impurities was routinely checked as described elsewhere.[18]

2.2. Methods. *2.2.1. Surface Pressure−Area Isotherms.* Compression isotherms at different temperatures were performed for ASC_{16}. A total of 25 μL of a solution of ASC_{16} was dissolved in a methanol/chloroform (1:1) mixture to obtain a solution of (1 mg/mL) total concentration, which was spread onto a 266 cm^2 Teflon trough filled with 200 mL of subphase. The aqueous solutions used as the subphase were (a) water, pH_b ∼ 6, (b) saline solution pH_b ∼ 6 (NaCl 145 mM), (c) saline solution pH_b ∼ 3 (NaCl 100 mM adjusted to pH3 with HCl), and (d) saline solution pH_b ∼ 8 (NaCl 90 mM TrisClH pH ∼ 8). The film was allowed to stand 5 min for solvent evaporation and monolayer relaxation at 0 mN/m, before being subsequently compressed isometrically (compression rate was between 1 and 3 $Å^2$ $molecule^{-1}$ min^{-1}, depending on the compressibility properties of the film) to the target pressure. The surface pressure was determined with a Pt plate using the Wilhelmy method, and the film total area was continuously measured and recorded using a KSV Minitrough apparatus (KSV, Helsinki, Finland) enclosed in an acrylic box which was previously enriched with N_2 gas. The subphase temperature (±0.5 °C) was controlled by an external circulation bath and kept at 25 °C unless indicated. A representative experiment is shown in all figures from a set of three independent experiments that differed in mean molecular area (MMA) and surface pressure measurements by less than 2 $Å^2$ and 0.2 mN m^{-1}, respectively.

In order to analyze the film elastic behavior of the adsorbed molecules, the compressibility modulus, C_s^{-1}, was calculated from the isotherm data as[19]

$$C_s^{-1} = -MMA\left(\frac{\partial \pi}{\partial MMA}\right)_T \quad (1)$$

where π represents the surface pressure. In order to prevent ASC_{16} oxidation, all measurements were performed maintaining an enriched N_2 atmosphere within the acrylic enclosure.[20]

2.2.2. Brewster Angle Microscopy (BAM) Measurements. The monolayers were prepared as described above using a model 102M apparatus (NIMA Technology Ltd., Coventry, England). The Langmuir apparatus was mounted on the stage of a Nanofilm EP3 imaging elipsometer (Accurion, Goettingen, Germany) used in the BAM mode. Zero reflection was set with a polarized 532 λ laser incident on the bare aqueous surfaces at the experimentally calibrated Brewster angle (∼53.1°). After monolayer formation and compression, the reflected light was collected with a 10× objective. Under the required calibration, the gray level of each pixel of the BAM images is directly related to the square of the film thickness.[21]

2.2.3. Surface Potential Measurements. The volta surface potential (ΔV) at 25 °C was recorded upon compression of the monolayer spread on the aqueous subphases, as described above in a homemade circular trough Langmuir balance (Monofilmmeter). This was monitored using an air-ionizing ^{241}Am surface electrode placed ≈5 mm above the interface and an Ag/AgCl/Cl^- (3M) reference electrode dipped into the subphase.[22]

The surface potential measured for a charged surface is given by[19]

$$\Delta V = \frac{4\pi\mu_\perp}{MMA} + \psi_0 \quad (2)$$

where $\mu_\perp$ is the overall resultant surfactant dipole moment in the direction perpendicular to the interface and ψ_0 is the potential difference due to the ionic double layer between the surface and the bulk of the subphase solution. ψ_0 was calculated according to the Poisson−Boltzmann equation as described in ref 23 which allows the $\mu_\perp$ parameter to be calculated.

2.2.4. Ionization State of ASC_{16} as a Function of the Bulk pH. As already mentioned in the Introduction, a monolayer of charged molecules will lead to a double layer of ions, thus attracting protons to the surface and inducing a lowering of the surface pH (pH_s) as follows:[19]

$$pH_s = pH_b + F\psi_0/2.3RT \quad (3)$$

where F is the Faraday constant and RT is the thermal energy. ψ_0 is a function of the ionic strength and the surface charge density,[23] which in turn depends on pH_s. Since, on the other hand, pH_s depends on

ψ_0 (eq 3),[17] a mutual regulation is established introducing further complexity. Upon considering the Poisson−Boltzmann equation for the surface charge density, the following relationship between the degree of dissociation (α), ψ_0, and pH_b can be obtained:

$$0 = \sqrt{2RT\varepsilon\varepsilon_0}\left[\sum_i C_i^b \exp(-Fz\psi_0/RT) - \sum_i C_i^b\right]^{1/2} + \frac{F}{MMA}\left[\frac{K_a}{K_a + [H^+]_b \exp(-F\psi_0\alpha/RT)}\right] \quad (4)$$

where ε is the medium permittivity (80); ε_0 is the vacuum permittivity; C_i^b is the ion concentration in the bulk; K_a is the acidic dissociation constant; z is the ion charge and $[H^+]_b$ is the bulk concentration of protons. From eq 4, ψ_0 and α can be calculated numerically for each pH_b value, knowing all the other parameters.

3. RESULTS AND DISCUSSION

3.1. Temperature Dependence of the Phase Behavior of ASC_{16} Monolayers. Compression isotherms of ASC_{16} spread on saline solution $pH_b \sim 6$ showed a liquid-expanded (LE) phase at low molecular densities (high mean molecular areas, MMA) (Figure 2a) which was demonstrated by the corresponding low compressibility modulus values ($C_s^{-1} < 50$ mN/m; see Figure 2b). Upon compression and at low temperatures, a near-plateau region was observed, characteristic of a diffuse first-order phase transition (Figure 2a). The compressed phase showed C_s^{-1} values of ~200 mN/m (Figure 2b), indicating a liquid-condensed (LC) character.[24] Further compression led to collapse of the monolayer at high surface pressures (~65 mN/m), demonstrating the high stability of the film, at least at temperatures under ~20 °C.

As expected, the LE−LC phase transition pressure increased with temperature, similar to that of other systems.[25] On the other hand, the collapse pressure decreased above 20 °C (inset in Figure 2a), indicating a favoring for the collapsed phase. A similar behavior was observed when water was used as the subphase, but an enhanced stability was shown of the condensed phase at lower surface pressures, thereby lowering the transition pressures (see inset in Figure 2a). This difference is discussed below. The MMA at the collapse pressure (the minimum area that ACS_{16} molecules can occupy in a monolayer) had an average value of 20 ± 2 Å^2 molecule^{-1}. The comparison of this value with the calculated cross-sectional area of the ASC_{16} polar headgroup (21 Å^2 molecule^{-1})[8] suggests a tight packing of the ASC_{16} molecules at the surface in the LC phase.

3.2. Calculation of the Dissociation Fraction of ASC_{16} Monolayers as a Function of Bulk pH and Salt Concentration. Taking into account the acidic properties of the C_3−OH group of the ascorbic ring, we estimated the ionization fraction of the molecules at the monolayer surface (α) as a function of the bulk pH (pH_b), for ion concentrations of 290 and 1×10^{-3} mM in the subphase by considering the Poisson−Boltzmann equation for the surface charge density (see Experimental Section). The results of this calculation are shown in Figure 3. Since the molecular density increased with a decrease in MMA, an increasingly negative charge density was established upon compression of the partially dissociated ASC_{16} molecules which induces a double layer potential (ψ_0).[23] Following eq 3, a negative value of ψ_0 (induced by a negatively charged surface) leads to a reduction of the surface pH (pH_s) (Figure 3a) and the α value decreases upon compression (Figure 3b). This effect was

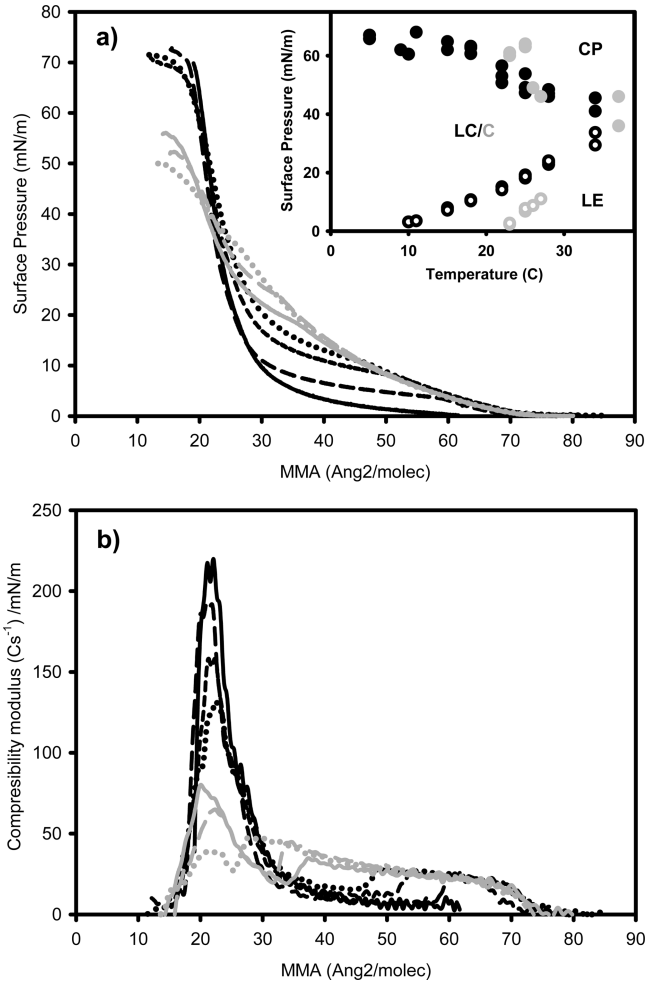

Figure 2. Surface behavior of ASC_{16} monolayers on saline solution $pH_b \sim 6$. (a) Compression isotherm and (b) compressibility modulus of ASC_{16} monolayers as a function of temperature as follows: 5 °C (black full line), 10 °C (long dashed line), 15 °C (short dashed line), 18 °C (dotted line), 25 °C (gray full line), 28 °C (gray dashed line), and 34 °C (gray dotted line). The figure shows representative curves from a set of three independent experiments. Inset in panel (a) shows the phase diagram for ASC_{16} monolayers using saline solution $pH_b \sim 6$ (black circles) and water (gray circles) as the subphase. LE corresponds to the liquid-expanded region, LC to the liquid-condensed and C to the crystalline one, and CP to the collapsed phase. Open circles indicate the beginning of the LE−LC or LE−C phase transition; closed circles indicate the collapse pressure. Each point corresponds to a single experiment.

particularly observed at $pH_b \sim 6$ and high salt conditions. This indicates that, during a compression isotherm, the surface charge density did not remain constant when working with a saline solution subphase, as shown in Figure 2. It is also shown in Figure 3 that when the monolayer was formed on a water surface with typically $pH_b \sim 6$, then the pH_s was predicted to be ~2.2 and the ASC_{16} molecules would be mostly present as neutral molecules ($\alpha \sim 1 \times 10^{-2}$). This finding may explain the differences observed in the phase diagram shown in the inset of Figure 2a. When ASC_{16} was present principally as a neutral molecule, the intermolecular interactions between the ascorbic rings may be favored and the condensed phase reached at lower surface pressures.

3.3. Phase and Monolayer Topography of ASC_{16} as a Function of Bulk pH and Salt Concentration. To investigate

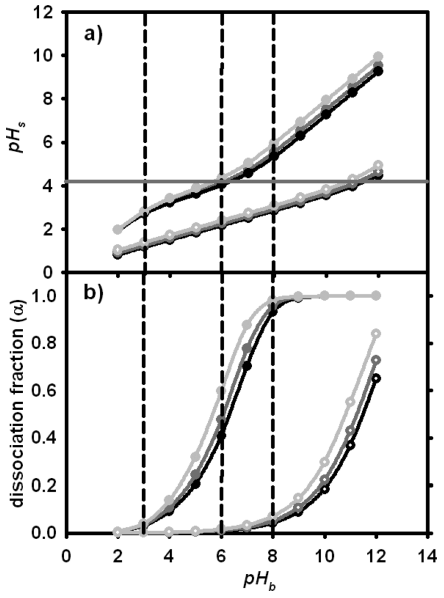

Figure 3. Ionization behavior of ASC_{16} at the interface. (a) Calculated pH at the surface and (b) calculated dissociation fraction of an acidic molecule of $pK_a = 4.2$ organized at the interface. The molecular density corresponds to a MMA of 65 (gray), 40 (dark gray) or 30 (black) $Å^2$ $molecule^{-1}$. The ion concentration of the subphase was 290 mM (closed circles) or 1×10^{-3} mM (open circles) at different bulk pHs. The horizontal gray line in (a) represents the ionization pK_a of ASC_{16}. The vertical dashed lines indicate bulk pH conditions further used in this work.

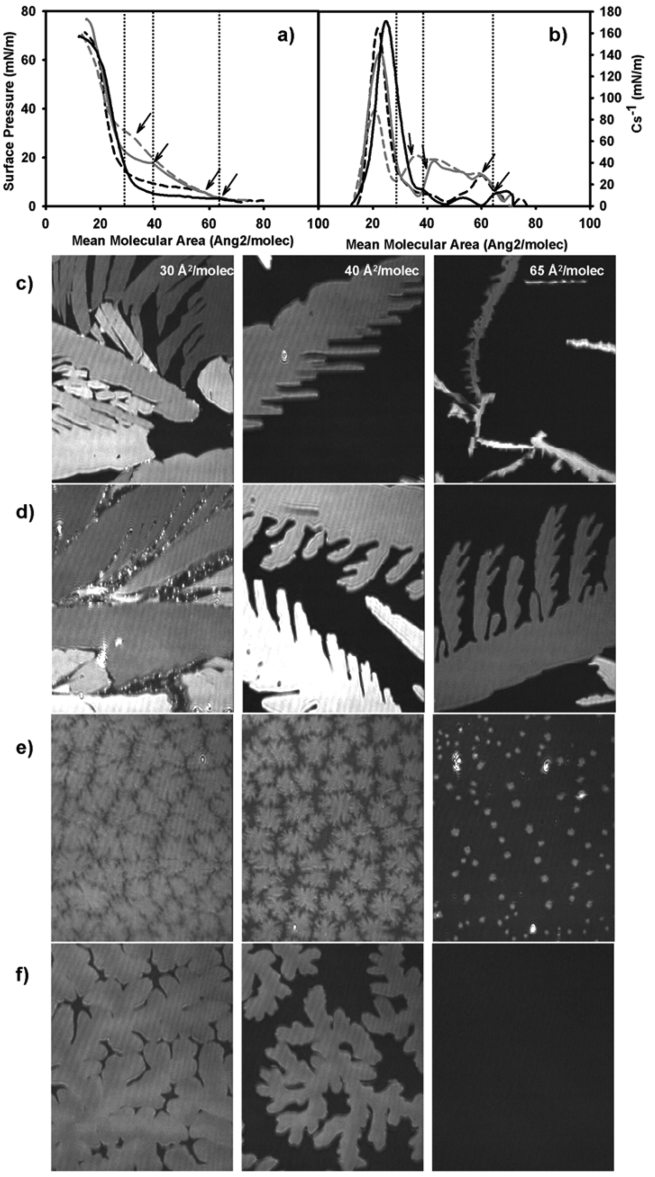

Figure 4. Surface behavior and topographic pattern of ASC_{16} monolayers on different subphases. (a) Compression isotherm and (b) compressibility modulus of ASC_{16} monolayers as a function of subphase conditions: saline solution $pH_b \sim 3$ (black full lines), water (black dashed lines), saline solution $pH_b \sim 6$ (gray full lines), and saline solution $pH_b \sim 8$ (gray dashed lines). The arrows indicate the beginning of the LE−condensed phase transition. The figure shows representative curves from a set of three independent experiments. Vertical dashed lines indicate the molecular density used for the calculations in Figure 3 and shown in images (c−f). Panels (c−f) show topographic pattern of ASC_{16} monolayers by BAM at the MMA indicated, using different surfaces: (c) water, (d) saline solution $pH_b \sim 3$, (e) saline solution $pH_b \sim 8$, and (f) saline solution $pH_b \sim 6$. For a better visualization, the lower 0−100 gray level range (from the 0−255 original scale) was selected in order to keep the gray level−film thickness relationship. The pictures are representative of two independent experiments. Image size 370×464 μm.

further the dependence of the ASC_{16} monolayer on subphase conditions, we also performed compression isotherms at different pH_b's and salt conditions at 25 °C and visualized the films by BAM. Figure 4 shows that the monolayers formed on the surface of a high salt subphase solution at $pH_b \sim 3$ exhibited similar features to the monolayers formed using water as the subphase (Figure 4a−d). For both conditions, the ASC_{16} molecules were predicted to be present principally in the neutral form (α in the 0.01−0.03 range) and therefore formed a low charge density interface (see Figure 3b). The BAM images of such films showed condensed domains with sharp edges that suggest a crystalline nature, with these domains growing upon compression. The cohesion of molecules into domains seemed to favor a defined direction at an angle of 39° ± 2° with the main domain axis. A second less developed branching, at 61° ± 2° from the main domain axis, was also observed in some cases (Figure 4c, d). Domains with similar textures have been previously reported for *N*-dodecyl-γ-hydroxybutiric acid amide (DHBAA) monolayers[26] with the principal growing direction at angles of 60°/30° ± 5°. These authors further demonstrated that the growing angles observed in the condensed domains responded to the lattice features of the crystalline structure.[27]

The BAM images shown in Figure 4c, d reveal different reflectivities of the neighboring domains (domains of different brightness). BAM studies also provide information on the molecular ordering of two-dimensional (2D) textures. When the alkyl chains are oriented parallel to the incident radiation plane, the *p*-polarized light is reflected without a change of polarization. However, if the domain is rotated, the brightness decreases with the azimuthal orientational order of the domain being in a direction other than that of the incident plane.[27−29] The ASC_{16} domains observed in Figure 4c, d show uniform reflectivity within each domain, suggesting a single orientation of the molecules forming a domain.

In the case when the calculations indicated a high α of ASC_{16} (saline solution $pH_b \sim 8$; see Figure 3), the LE phase remained

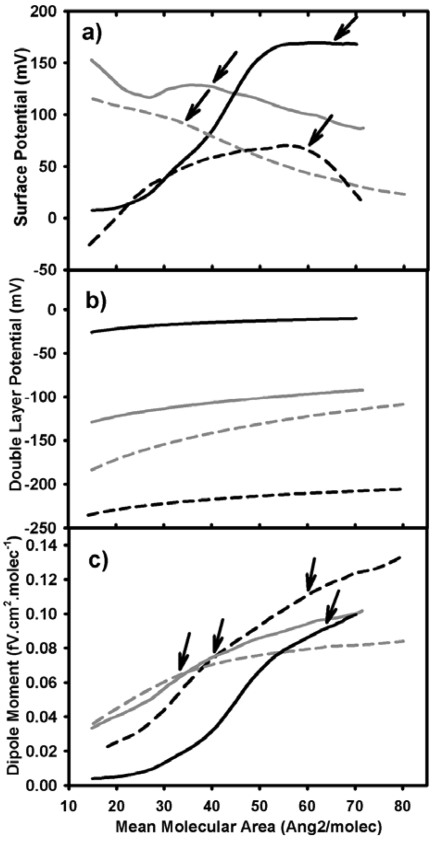

Figure 5. Surface potential behavior of ASC_{16} monolayers for different subphases. (a) Surface potential, (b) calculated double layer potential (from eq 4), and (c) calculated resultant perpendicular dipole moment (from eq 2, see Experimental Section) of ASC_{16} monolayers as a function of subphase composition: saline solution $pH_b \sim 3$ (black full lines), water $pH_b \sim 6$ (black dashed lines), saline solution $pH_b \sim 6$ (gray full lines), and saline solution $pH_b \sim 8$ (gray dashed lines). The arrows indicate the beginning of the LE−condensed phase transition upon compression. Panel (a) shows representative experimental curves from a set of three independent experiments that differed by less than 20 mV.

stable up to high surface pressures (~30 mN/m), as shown by the compression isotherm (Figure 4a). Then, upon further compression, a LC phase that had a lower compressibility modulus (compared to that of the crystalline phase observed for other subphase conditions, Figure 4b) was seen. The LC phase had a pattern of smaller domains with highly undulated borders and a uniform gray level (Figure 4e), indicating a 2D isotropic system. This means that ionization of ASC_{16} at the surface likely involved intermolecular repulsions that favored a more expanded phase and impaired formation of crystalline domains. An intermediate behavior was observed in the isotherms and the BAM images for monolayers of ASC_{16} on saline solutions at $pH_b \sim 6$ (Figure 4a, b, and f), with our calculations predicting an α value of ~0.5 (see also Figure 3). Under these conditions, the LC phase showed larger domains with less undulated borders.

3.4. Surface Potential and Perpendicular Dipole Moment Calculation. To understand further the behavior of the ASC_{16} monolayers, we performed measurements of surface potential (ΔV) as a function of the packing density. Figure 5a shows the change in ΔV upon compression, measured for the ASC_{16} monolayers in different subphase conditions. The potential difference due to the ion double layer (ψ_0) was calculated for each subphase condition as a function of MMA (Figure 5b) using eq 4. This permits the estimation of the resultant perpendicular dipole moment ($\mu_\perp$) of the ASC_{16} molecules using eq 2, as shown in Figure 5c. The calculation of ψ_0 (Figure 5b) resulted in values that increased in the sequence: saline $pH_b \sim 3$ < saline $pH_b \sim 6$ < saline $pH_b \sim 8$ < water $pH_b \sim 6$. Considering only saline solutions, we found, as expected,[17] that the larger the α at the surface (and therefore the higher the charge density), the higher the ψ_0 value (see Figures 3b and 5b). For the ASC_{16} monolayer on a water subphase, the calculated α was only 0.01 at a MMA of 40 $Å^2$/molecule. Even if this were considered as an essential "neutral monolayer" in the case of the experiments in Figure 4, it still behaved as a charged surface when considering ψ_0. Therefore, when there was an ion concentration of only 1×10^{-6} M (the proton concentration in pure water at $pH_b \sim 6$) to counteract the electrostatic potential induced by 1% of the ASC_{16} molecules charged, ψ_0 attained higher negative values than in any other conditions assayed (Figure 5b).

Since ΔV is dependent on both, the packing density and the orientation of the molecules in the monolayer (see eq 2), we expected a rise in the ΔV values during compression of the LE phases as a consequence of a progressive standing up toward a vertical position, which was observed for the charged monolayers (on saline solution of pH_b of ~6 and 8) at low packing densities (Figure 5a). When the monolayers were in an LC state (low MMA range), the ΔV values rose to 100−150 mV. This difference in ΔV between both phases of the charged monolayers ($\Delta V_{LC} - \Delta V_{LE}$) may account for intradomain repulsions leading to the flowerlike domain shapes,[30] as observed by BAM (Figure 4e, f). The analysis of Figure 5c shows a continuous monotonic decrease in $\mu_\perp$ for the charged monolayers, which may indicate compensation of the internal molecular dipoles and/or changes in the hydration/ion interaction as a consequence of compression. The "neutral monolayers" (in water and saline solution pH_b3) had a more pronounced reorganization of ΔV and $\mu_\perp$, from higher to lower values, which coincided with the phase transition region. As a consequence, the overall resultant $\mu_\perp$ fell to a value close to zero when the monolayer was in the crystalline state (low MMA values), suggesting a compensation/reorientation of the fundamental dipoles of the molecule, changes in the hydration of the polar headgroup, or a combination of these effects.

4. CONCLUSIONS

ASC_{16} self-organizes into Langmuir monolayers with electrostatic properties being highly dependent on the subphase pH and salt conditions. In the present work, we investigated theoretically and experimentally the morphological and thermodynamic changes induced by alteration of the charge density of the ASC_{16} monolayers by dissociation of the acidic C_3−OH of the ascorbic ring. A highly packed film of ASC_{16} molecules was revealed from measurements of the mean molecular area close to the minimal theoretical one. Also a tilted, uniform ordering of the molecules within the domains was suggested by the different reflectivities observed by BAM in the neighboring domains, in conditions of low dissociation. These properties and the preferential growth of the domains at characteristic angles strongly suggest a crystalline nature of the condensed domains grown in conditions of low dissociation. On the other hand, isotropic flowerlike domains, probably induced by high intradomain

repulsion, were formed by compression of the charged monolayer. Taken together, these results demostrate the rich complexity of surface phenomena arising from the interplay of a charged self-assembled structure that showed a dynamic 2D organization with the bulk ionic response. Additionally, this study contributes to a deeper understanding and molecular control of the properties of ASC_{16} as a potential tool for pharmaceutical formulations.

AUTHOR INFORMATION

Corresponding Author

*Telephone: +54 351 4334168. Fax: +54 351 4334074. E-mail: lfanani@fcq.unc.edu.ar.

ACKNOWLEDGMENT

This work was supported by the Universidad Nacional del Sur, Agencia Nacional de Promoción Científica y Tecnológica (FONCyT), Consejo Nacional de Investigaciones Científicas y Técnicas de la República Argentina (CONICET), SECyT-Universidad Nacional de Córdoba and Agencia Córdoba Ciencia -MinCyT (Córdoba). M.L.F, N.W., B.M, P.M., and S.P. are Career Researchers of CONICET. L.B. has a fellowship from CONICET.

ABBREVIATIONS

ASC_{16}, ascorbyl palmitate; MMA, mean molecular area; ΔV, surface potential; $\mu_{\perp}$, perpendicular dipole moment; ψ_0, double layer potential; LE, liquid-expanded; LC, liquid-condensed; CP, collapsed phase; pH_b, bulk pH; pH_s, surface pH; BAM, Brewster angle microscopy

REFERENCES

(1) Keller, K. L.; Fenske, N. A. *J. Am. Dermatol.* **1998**, *39*, 611–625.
(2) Philips, C. L.; Combs, S. B.; Pinell, S. *J. Invest. Dermatol.* **1994**, *103*, 227–234.
(3) Colven, R. M.; Pinnell, S. R. *Clin. Dermatol.* **1996**, *14*, 227–234.
(4) Austria, R.; Semenzazo, A.; Bettero, A. *J. Pharm. Biomed. Anal.* **1997**, *15*, 795–801.
(5) Palma, S.; Lo, N. P.; Manzo, R.; Allemandi, D. *Eur. J. Pharm. Sci.* **2002**, *16*, 37–43.
(6) Palma, S. D.; Maletto, B.; Lo, N. P.; Manzo, R. H.; Pistoresi-Palencia, M. C.; Allemandi, D. A. *Drug Dev. Ind. Pharm.* **2006**, *32*, 821–827.
(7) Spiclin, P.; Gasperlin, M.; Kmetec, V. *Int. J. Pharm.* **2001**, *222*, 271–279.
(8) Palma, S.; Manzo, R.; Lo, N. P.; Allemandi, D. *Int. J. Pharm.* **2007**, *345*, 26–34.
(9) Lo, N. P.; Ninham, B.; Fratoni, L.; Palma, S.; Manzo, R.; Allemandi, D.; Baglioni, P. *Langmuir* **2003**, *19*, 3222–3228.
(10) Palma, S.; Manzo, R. H.; Allemandi, D.; Fratoni, L.; Lo, N. P. *J. Pharm. Sci.* **2002**, *91*, 1810–1816.
(11) Palma, S.; Manzo, R.; Allemandi, D.; Fratoni, L.; Lo, N. P. *Colloids Surf., A* **2003**, 212–163.
(12) Martin, A. N.; Bustamante, P. *Physical Pharmacy: Physical Chemistry Principles in the Pharmaceutical Science*, 4th ed.; Lea & Febiger: Philadelphia, 1993.
(13) Capuzzi, G.; Lo, N. P.; Kulkarni, K.; Fernandez, J. E.; Vincieri, F. F. *Langmuir* **1996**, *12*, 5413–5418.
(14) Minardi, R. M.; Schulz, P.; Vuano, B. *Colloid Polym. Sci.* **1997**, *275*, 754–759.
(15) Benedini, L.; Schulz, E. P.; Messina, P.; Palma, S.; Allemandi, D.; Schulz, P. *Colloids Surf.,A* **2011**, *375*, 178–185.
(16) Martindale, P. K. *The Complete Drug Reference*, 34th ed.; The Pharmaceutical Press: London, 2005.
(17) Tocanne, J. F.; Teissie, J. *Biochim. Biophys. Acta* **1990**, *1031*, 111–142.
(18) Bianco, I. D.; Maggio, B. *Colloids Surf.* **1989**, *40*, 249–260.
(19) Gaines, G. L. *Insoluble monolayers at liquid-gas interfaces*; Interscience Publishers: New York, 1966.
(20) Brown, R. E.; Brockman, H. L. *Methods Mol. Biol.* **2007**, *398*, 41–58.
(21) Fanani, M. L.; Maggio, B. *J. Phys. Chem. B* **2011**, *115*, 41–49.
(22) Wilke, N.; Maggio, B. *J. Phys. Chem. B* **2009**, *113*, 12844–12851.
(23) Mercado, F. V.; Maggio, B.; Wilke, N. *Chem. Phys. Lipids* **2011**, *164*, 386–392.
(24) Davies, J. T.; Rideal, E. K. *Interfacial Phenomena*; Academic Press: New York, 1963.
(25) Fanani, M. L.; Maggio, B. *Chem. Phys. Lipids* **2010**, *163*, 594–600.
(26) Vollhardt, D.; Melzer, V. *J. Phys. Chem. B* **1997**, *101*, 3370–3375.
(27) Vollhardt, D.; Fainerman, V. B. *Adv. Colloid Interface Sci.* **2010**, *154*, 1–19.
(28) Overbeck, G. A.; Honig, D.; Wolthaus, L.; Gnade, M.; Mobius, D. *Thin Solid Films* **2011**, *242*, 26–32.
(29) Angelova, A.; Vollhardt, D.; Ionov, R. *J. Phys. Chem.* **1996**, *100*, 10710–10720.
(30) McConnell, H. M. *Annu. Rev. Phys. Chem.* **1991**, *42*, 171–195.